A Lateral Positioning Strategy for Connected and Automated Vehicles in Lane-free Traffic

Ioannis Faros[1], Venkata Karteek Yanumula[1], Panagiotis Typaldos[1], Ioannis Papamichail[1], Markos Papageorgiou[1,2]

[1] Dynamical System and Simulation Laboratory, Technical University of Crete, Chania, Greece,

[2] Faculty of Maritime and Transportation, Ningbo University, Ningbo, China

Abstract

An optimal-control based path planning algorithm has been developed recently for Connected and Automated Vehicles (CAVs) driving on a lane-free highway, including vehicle nudging. That vehicle movement strategy considers, in the lateral direction, a lateral desired speed that had been set to zero in previous works; in other words, vehicles avoid lateral movement if this is not helpful in achieving some of their goals, e.g. achieving a longitudinal desired speed by overtaking slower vehicles. In this work, a lateral positioning strategy for the vehicles is proposed, aiming to improve the vehicles' longitudinal speeds and the traffic flow, mainly at intermediate densities, by distributing laterally the vehicles based on their longitudinal desired speeds. The intention is to leverage the existing optimal control formulation to move the CAVs to appropriate lateral positions, while respecting other, higher-priority sub-objectives, such as avoiding crashes. First, the longitudinal desired speed of each vehicle is mapped to a lateral desired position under the premise "faster vehicles drive farther left". Then, the value of the desired lateral speed is updated in real-time in dependence on the vehicle's current versus the desired lateral position, letting the optimal control problem, with the given sub-objective priorities, decide on the actual vehicle path. The proposed strategy is demonstrated via traffic simulations, involving various traffic densities, on a ring-road. Several quantities, such as the reached average flows and statistical measures of the error in the lateral position are computed for evaluation and comparison purposes.

Keywords: automated vehicles, lane-free traffic, lateral control strategy

1 Introduction

Automation has enhanced production and reduced errors in a wide range of applications. Automation in vehicular traffic comprising Connected and Automated Vehicles (CAVs) is predicted to provide similar outcomes [Dia15; Sjo17]. In this context, some road safety rules designed for human drivers with limited perception and decision capabilities, such as driving strictly on traffic lanes or driving based only on downstream perception, may be questioned. Technologies, like vehicle automation, as well as vehicle-to-vehicle (V2V) and vehicle-to-infrastructure (V2I) communication, have the potential to improve road safety and traffic flow greatly, by relaxing such constraints designed for human drivers.

Road driving is moving in the direction of complete automation and cooperation of CAVs. According to a recently proposed, novel traffic paradigm [Pap21], there is no need, in the era of CAVs to duplicate the human lane-based and forward-looking driving. Based on appropriate movement strategies, in combination with advanced vehicle sensors and communications, CAVs may navigate securely and efficiently on the two-dimensional road surface, accounting for other vehicles all around them, the latter leading to the notion of vehicle nudging.

Alongside various strategies [Tro21a; Kar22], the work by [Yan21; Yan23] formulated a nonlinear Optimal Control Problem (OCP) for CAV path planning in lane-free traffic with nudging. The OCP considers minimization of an objective function that involves fuel consumption, passenger comfort, moving obstacle avoidance, and desired speeds. A feasible direction algorithm is used for its computationally efficient numerical solution [Pap16]. This paper leverages the OCP approach to enable consideration of a target lateral position for each vehicle.

The developed strategy aims to improve longitudinal vehicle speeds and thereby the traffic mean speed and flow, mainly at under-critical traffic densities, where vehicle maneuvering is easier. This is to be achieved by distributing laterally the vehicles, based on their longitudinal desired speeds, so that vehicles with higher desired speed tend to drive further left (and vice versa). This work leverages the OCP formulation to include an additional sub-objective for moving the CAVs to a desired lateral position on the road, while respecting other sub-objectives with higher priority, such as avoiding collisions. The proposed approach is demonstrated to give good results in a simulation environment, for a range of under-critical traffic densities on a lane-free ring-road and can be considered for use in future advancements linked to lane-free CAV traffic.

2 Methodology

The movement of the q^{th} vehicle in the two-dimensional plane is described by the double-integrator kinematic equations in both longitudinal and lateral directions, whereby the control inputs are the accelerations in both directions. The state equations are the following:

$$x_1^q(k+1) = x_1^q(k) + Tx_3^q(k) + \frac{1}{2}T^2u_1^q(k), \tag{1}$$

$$x_3^q(k+1) = x_3^q(k) + Tu_1^q(k), \tag{2}$$

$$x_2^q(k+1) = x_3^q(k) + Tx_4^q(k) + \frac{1}{2}T^2u_2^q(k), \tag{3}$$

$$x_4^q(k+1) = x_4^q(k) + Tu_2^q(k), \tag{4}$$

where the state variables $x_1^q, x_2^q, x_3^q, x_4^q$ represent the longitudinal position, the lateral position, the longitudinal speed, and the lateral speed, respectively, while the control variables u_1^q, u_2^q represent the longitudinal and the lateral accelerations, respectively. T is the time step, and k is the discrete-time index, which relates to the continuous time through $t = kT$. The CAVs are essentially advancing in the longitudinal direction within the lateral road boundaries.

Preventing road departures and negative longitudinal speeds and avoiding collisions in some "emergency situations" are defined as state-dependent inequality constraints on accelerations, to be considered in the OCP. The objective function to be minimized is composed of several sub-objectives. Fuel consumption [Typ20] and passenger comfort, reaching desired speeds in both directions, obstacle avoidance in regular situations, coupling of longitudinal and lateral speeds and smooth longitudinal acceleration between planning horizons are the sub-objectives composing the total objective function; see [Yan21; Yan23] for details.

In summary, the OCP minimizes the overall objective function, subject to the state equations (1) – (4) and all constraints. The OCP can be transformed into a nonlinear programming problem in the reduced space of control variables. Using an efficient feasible direction algorithm [Pap15; Pap16], the OCP is solved repeatedly for short time horizons within a model predictive control (MPC) framework, while the vehicle advances.

In [Yan21; Yan23], the OCP objective includes a lateral desired speed that is set to zero to discourage unnecessary lateral movements of the vehicle. We consider this to be the base case strategy (BCS) for comparison purposes. In the present work, a new lateral positioning strategy (LPS) is proposed that pursues the premise "faster vehicles drive farther left", similarly to conventional traffic, albeit without the presence of traffic lanes.

Note that the admissible lateral positions for a vehicle in lane-free traffic are within the road boundaries, i.e. within the range $[W_v/2, W_r - W_v/2]$, where W_v is the width of the vehicle and W_r is the width of the road, as illustrated in Figure 1.

For the present investigations, each vehicle features a longitudinal desired speed (x_{3des}^q) from the range $[a, b]$ m/s, assigned with a uniform random distribution. Other desired speed distributions are currently under investigation. In the case of homogeneous distribution, we may use a linear mapping that returns a desired lateral position (x_{2des}^q), proportional to the desired speed, by the following equation

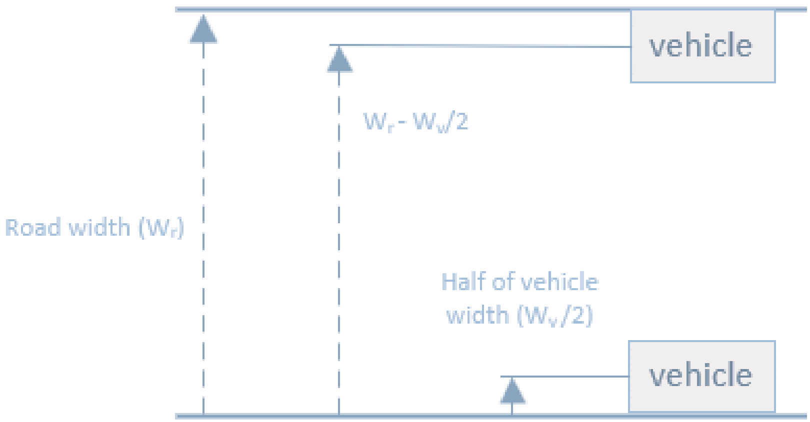

Figure 1: Lateral road boundaries and admissible vehicle positions.

$$x^q_{2des} = \left(W_r - \frac{W_v}{2} - \frac{W_v}{2}\right)\left(\frac{x^q_{3des} - a}{b-a}\right) + \frac{W_v}{2},\ \forall x^q_{3des} \in [a,b]. \tag{5}$$

Equation (5) is performing a one-to-one mapping between the two intervals:

$$[a,b] \to \left[\frac{W_v}{2}, W_r - \frac{W_v}{2}\right].$$

This way, each vehicle is assigned a desired lateral position, and it should tend to approach that position, as it drives on the road. Although we could formulate this task as an additional sub-objective in the OCP objective function, we prefer, for the sake of simplicity and generality, to address this task by leveraging the existing lateral desired speed term in the objective function. This implies that, at each optimization run, we need to update the desired lateral speed to conform with the lateral position task. This is done by computing the lateral desired speed proportionally (according to (6)) to the vehicle deviation from the desired lateral position at the start of each OCP run. More precisely, the lateral speed, that should be applied to the vehicle over a time-period S to reach its desired position, is simply given by $(x^q_{2des} - x^q_2(0))/S$ (where $x^q_2(0)$ is its initial lateral position) and is used as its desired lateral speed

$$x^q_{4des} = \frac{x^q_{2des} - x^q_2(0)}{S}. \tag{6}$$

3 Results and Discussion

An unfolded ring-road of 1 km length and 10.2 m width is considered for simulations in a lane-free environment. Multiple scenarios have been simulated using a custom-made extension, namely TrafficFluid-Sim [Tro21b], which is built for the SUMO simulator [Lop18]. Eight classes of regular vehicles are included, each class with its own length and width, as follows (in m): (3.2,1.6), (5.15,1.84), (4.25,1.8), (4.55,1.82), (2.6,1.77), (3.9,1.7), (3.4,1.7), and (5.2,1.88). The longitudinal desired speeds are set randomly, following the uniform distribution, in the range [25,35] m/s. Initially, each vehicle is placed randomly, in lateral direction, within the range $[W_v/2, W_r - W_v/2]$; while longitudinal initial positions are roughly homogeneously distributed; and initial speeds are 0. The optimization horizon is set to 8 sec with a simulation step of 0.25 sec. A time-period S of 32 sec is used in (6) so as to reach the desired lateral position in four optimization horizons.

To evaluate the scenarios, the average flows achieved during the last ten minutes of half-hour simulations and the statistics of the lateral-position error throughout the simulation period are calculated. The average Mean Absolute Error (Average-MAE) between the current lateral position and the desired lateral position for all time steps and for all vehicles is calculated using the following formula

$$\text{Average} - \text{MAE} = \frac{1}{n}\sum_{q=1}^{n}\left(\frac{1}{tnss}\sum_{i=1}^{tnss}|x_2^q(i) - x_{2des}^q(i)|\right), \tag{7}$$

where $tnss$ is the total number of simulation steps and n is the number of vehicles. The standard deviation of the MAE (stdv-MAE) is calculated based on the following formula

$$\text{stdv} - \text{MAE} = \sqrt{\frac{1}{n}\sum_{q=1}^{n}\left[\frac{1}{tnss}\sum_{i=1}^{tnss}\left[|x_2^q(i) - x_{2des}^q(i)| - \text{Average} - \text{MAE}\right]^2\right]}. \tag{8}$$

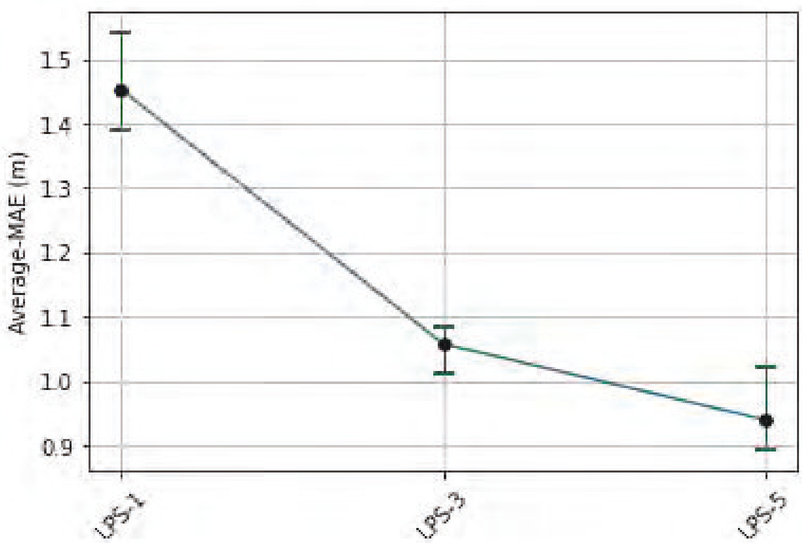

Figure 2: Average-MAE for three different values of the weight applied on the lateral desired speed term. The bars represent the range of values over the 5 different replications.

First, an investigation has been conducted using different values for the weight applied on the penalty term corresponding to the squared deviation from the lateral desired speed. Different values have been considered for this weight to explore its impact on the flow and on the deviation from the desired lateral position via the metrics (7) – (8), while also looking at its impact on other sub-objectives. As expected, an increase of the weight results in a decrease of the Average-MAE. This is shown in Figure 2, which displays the average and the range of values achieved over 5 different replications for the case of a density equal to 150 veh/km and for three different values (1, 3 and 5) used for the weight. Figure 3 shows the stdv-MAE value for the same density and again for the three different values used for the weight. In all cases, the flow achieved with the proposed LPS is improved, compared to the flow achieved for the BCS (see Figure 4 and Table 1). On average, this improvement is higher for higher values of the weight. However, according to Figure 4, the deviation from the average flow value that is observed over the 5 replications is much higher for the case of a weight equal to 5. Therefore, the value of the weight considered in the following investigations with different densities is selected to be equal to 3.

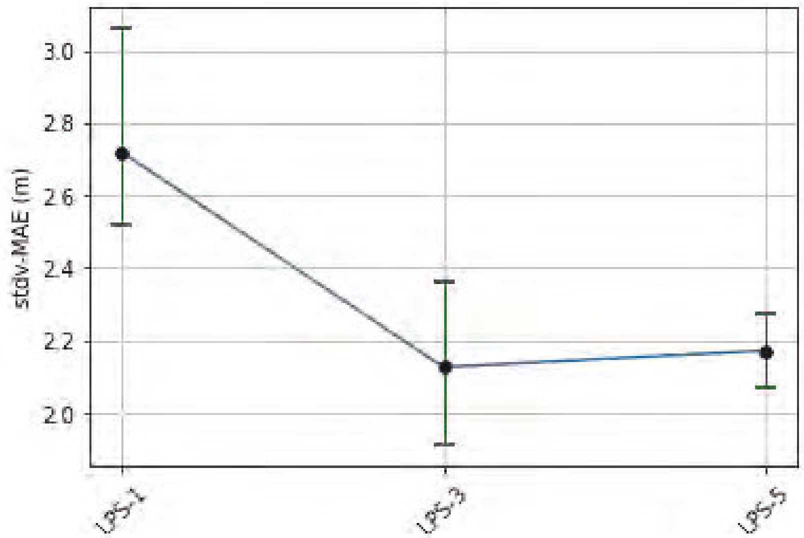

Figure 3: stdv-MAE for three different values of the weight applied on the lateral desired speed term. The bars represent the range of values over the 5 different replications.

Table 1: Flow Improvement achieved over the BCS for different values of the weight applied on the lateral desired speed term.

Weight	1	3	5
Flow Improvement (%)	4.45	4.73	4.89

The average flows achieved during the last ten minutes of half-hour simulations for different densities and 5 replications per density are used to plot the resulting fundamental diagram given in Figure 5. The same diagram includes the flows achieved for the BCS, i.e. when using the policy of zero lateral desired speed, utilized by [Yan21; Yan23]. The bars represent the range of values over the 5 replications. We observe that the critical density is 200 veh/km, while the proposed LPS improves flows around the critical density area (see Table 2 for the improvements achieved). Note that the proposed strategy has virtually no ef-

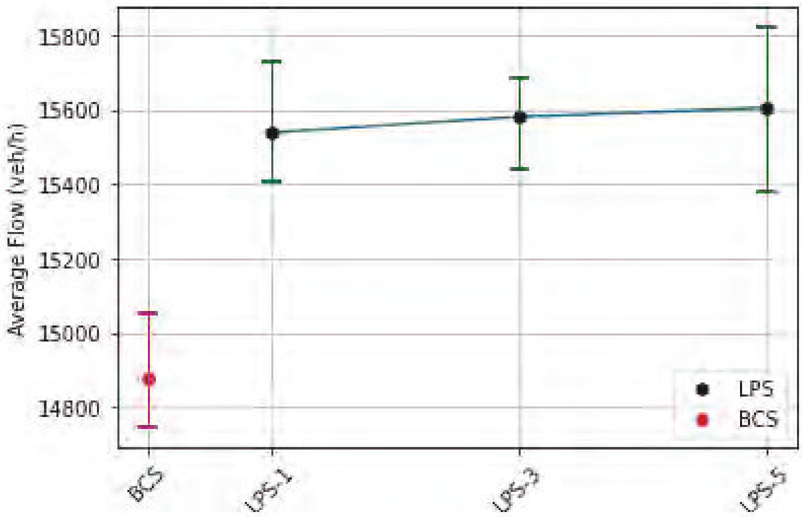

Figure 4: Average flow for the BCS and the LPS for three different values of the weight applied on the lateral desired speed term. The bars represent the range of values over the 5 different replications.

fect for very low and overcritical densities. For the case of very low densities, this is because the vehicles have anyway the space necessary to overtake slower vehicles and, as a result, they are able to achieve their desired speed. On the other hand, for overcritical densities, there is little space for maneuvers, hence the new strategy does not offer any visible advantage. Finally, for very high densities, a flow decrease is observed when using the proposed strategy. This is due to a high number of emergency situations occurring in higher densities, probably due to the additional lateral movements caused by the new sub-objective. Thus, one may consider applying LPS only around the critical density, where improvements are pronounced.

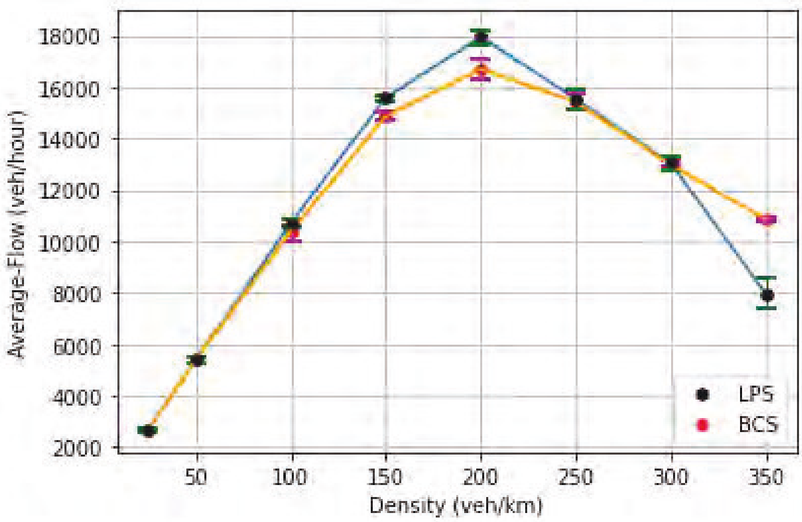

Figure 5: Fundamental diagram for the BCS and the LPS. The bars represent the range of values over the 5 different replications.

Table 2: Flow improvement achieved over the BCS per density.

Density (veh/km)	25	50	100	150	200	250	300	350
Flow Improvement (%)	-0.04	0.27	3.65	4.73	7.47	0.81	0.47	-26.60

4 Conclusions

A lateral control approach is developed for CAVs to reach a desired lateral position according to the desired longitudinal speed, with an aim to segregate similar longitudinal speed vehicle in the lateral space. It is demonstrated via SUMO on a ring-road for various densities that, when the proposed LPS is applied, the traffic flow is increased for densities around the critical area. The impact of the weight of the lateral desired speed term is also investigated. Future work is focused on having a non-homogeneous distribution in the road (including trucks), and introducing on-ramps, off-ramps, where lateral desired speeds have also a major role to enable merging and exiting of vehicles.

Acknowledgements

The research leading to these results has received funding from the European Research Council under the European Union's Horizon 2020 Programme / ERC Grant Agreement no. 833915, project TrafficFluid, see: `https://www.trafficfluid.tuc.gr`.

References

[Dia15] C. Diakaki, M. Papageorgiou, I. Papamichail, and I. Nikolos: "Overview and analysis of vehicle automation and communication systems from a motorway traffic management perspective". In: *Transportation Research: Part A* 75 (May 2015), pages 147–165. issn: 0965-8564. doi: 10.1016/j.tra.2015.03.015.

[Kar22] I. Karafyllis, D. Theodosis, and M. Papageorgiou: "Constructing artificial traffic fluids by designing cruise controllers". In: *Systems & Control Letters* 167 (Mar. 2022). issn: 0167-6911. doi: 10.1016/j.sysconle.2022.105317.

[Lop18] P. A. Lopez, M. Behrisch, L. Bieker-Walz, J. Erdmann, Y. P. Flötteröd, R. Hilbrich, L. Lücken, J. Rummel, P. Wagner, and E. Wiessner: "Microscopic Traffic Simulation using SUMO". In: *2018 International Conference on Intelligent Transportation Systems (ITSC)*. Edited by W.-B. Zhang, A. M. Bayen, J. J. S. Medina, and M. J. Barth. Institute of Electrical and Electronics Engineers, Nov. 2018, pages 2575–2582. doi: 10.1109/ITSC.2018.8569938.

[Pap15] M. Papageorgiou, M. Leibold, and M. Buss: *Optimierung. statische, dynamische, stochastische Verfahren für die Anwendung*. Berlin, Heidelberg: Springer, 2015. isbn: 978-3-66-246936-1.

[Pap16] M. Papageorgiou, M. Marinaki, P. Typaldos, and K. Makantasis: *A feasible direction algorithm for the numerical solution of optimal control problems-extended version*. Technical report. Internal Report 26. Dynamic Systems and Simulation Laboratory, Technical University of Crete, 2016.

[Pap21] M. Papageorgiou, K.-S. Mountakis, I. Karafyllis, I. Papamichail, and Y. Wang: "Lane-free artificial-fluid concept for vehicular traffic". In: *Proceedings of the IEEE*. Volume 109. Institute of Electrical and Electronics Engineers, Feb. 2021, pages 114–121. DOI: 10.1109/jproc.2020.3042681.

[Sjo17] K. Sjoberg, P. Andres, T. Buburuzan, and A. Brakemeier: "Cooperative intelligent transport systems in europe: Current deployment status and outlook". In: *IEEE Vehicular Technology Magazine* 12 (June 2017), pages 89–97. ISSN: 1556-6072. DOI: 10.1109/mvt.2017.2670018.

[Tro21a] D. Troullinos, G. Chalkiadakis, I. Papamichail, and M. Papageorgiou: "Collaborative multiagent decision making for lane-free autonomous driving". In: *2021 International Conference on Autonomous Agents and Multiagent Systems (AAMAS)*. Edited by F. Dignum, A. Lomuscio, U. Endriss, and A. Nowé. Virtual Event, United Kingdom: ACM, May 3–7, 2021, pages 1335–1342.

[Tro21b] D. Troullinos, G. Chalkiadakis, D. Manolis, I. Papamichail, and M. Papageorgiou: "Lane-Free Microscopic Simulation for Connected and Automated Vehicles". In: *2021 IEEE International Conference on Intelligent Transportation Systems Conference (ITSC)*. Indianapolis, USA: Institute of Electrical and Electronics Engineers, Sept. 19–22, 2021, pages 3292–3299. DOI: 10.1109/ITSC48978.2021.9564637.

[Typ20] P. Typaldos, I. Papamichail, and M. Papageorgiou: "Minimization of Fuel Consumption for Vehicle Trajectories". In: *IEEE Transactions on Intelligent Transportation Systems* 21.4 (2020), pages 1716–1727. ISSN: 1524-9050. DOI: 10.1109/TITS.2020.2972770.

[Yan21] V. K. Yanumula, P. Typaldos, D. Troullinos, M. Malekzadeh, I. Papamichail, and M. Papageorgiou: "Optimal Path Planning for Connected and Automated Vehicles in Lane-free Traffic". In: *2021 IEEE International Conference on Intelligent Transportation Systems Conference (ITSC)*. Institute of Electrical and Electronics Engineers, Sept. 19–22, 2021, pages 3545–3552. DOI: 10.1109/ITSC48978.2021.9564698.

[Yan23] V. K. Yanumula, P. Typaldos, D. Troullinos, M. Malekzadeh, I. Papamichail, and M. Papageorgiou: "Optimal Trajectory Planning for Connected and Automated Vehicles in Lane-free Traffic with Vehicle Nudging". In: *IEEE Transactions on Intelligent Vehicles* (2023), pages 1–15. DOI: 10.1109/tiv.2023.3241200.

Corresponding author: Ioannis Papamichail, Dynamical System and Simulation Laboratory, Technical University of Crete, Chania, Greece, e-mail: ipapa@dssl.tuc.gr